ELSEVIER

Biophysical Chemistry 92 (2001) 17–34

Biophysical Chemistry

www.elsevier.com/locate/bpc

A model of oxidative phosphorylation in mammalian skeletal muscle

Bernard Korzeniewski[a,*], Jerzy A. Zoladz[b]

[a] *Institute of Molecular Biology, Jagiellonian University, al. Micjkiewicza 3, 31-120 Kraków, Poland*
[b] *Department of Physiology and Biochemistry, Institute of Human Physiology, AWF, Kraków, Poland*

Received 29 January 2001; received in revised form 2 May 2001; accepted 29 May 2001

Abstract

A dynamic computer model of oxidative phosphorylation in oxidative mammalian skeletal muscle was developed. The previously published model of oxidative phosphorylation in isolated skeletal muscle mitochondria was extended by incorporation of the creatine kinase system (creatine kinase plus phosphocreatine/creatine pair), cytosolic proton production/consumption system (proton production/consumption by the creatine kinase-catalysed reaction, efflux/influx of protons), physiological size of the adenine nucleotide pool and some additional minor changes. Theoretical studies performed by means of the extended model demonstrated that the CK system, which allows for large changes in P_i in relation to isolated mitochondria system, has no significant influence on the kinetic properties of oxidative phosphorylation, as inorganic phosphate only slightly modifies the relationship between the respiration rate and [ADP]. Computer simulations also suggested that the second-order dependence of oxidative phosphorylation on [ADP] proposed in the literature refers only to the ATP synthesis flux, but not to the oxygen consumption flux (the difference between these two fluxes being due to the proton leak). Next, time courses of changes in fluxes and metabolite concentrations during transition between different steady-states were simulated. The model suggests, in accordance with previous theoretical predictions, that activation of oxidative phosphorylation by an increase in [ADP] can (roughly) explain the behaviour of the system only at low work intensities, while at higher work intensities parallel activation of different steps of oxidative phosphorylation is involved.

Keywords: Computer model; Energy metabolism; Mitochondrial respiration

* Corresponding author. Tel.: +48-12-341305, ext. 285: fax: +48-12-336907.
E-mail address: benio@mol.uj.edu.pl (B. Korzeniewski).

0301-4622/01/$ - see front matter
PII: S0301-4622(01)00184-3

1. Introduction

Oxidative phosphorylation is the main process responsible for the production of energy in the form of ATP in oxidative skeletal muscle under most conditions. The entire general sequence of biochemical events leading to the synthesis of ATP in the process of oxidation of respiratory substrates has been known since Mitchell proposed his chemiosmotic theory [1,2]. However, the way in which the oxidative phosphorylation system is regulated in intact tissues still remains a matter of debate.

Great changes in ATP demand take place in skeletal muscle during transition from resting state to intensive exercise. To avoid a quick depletion of ATP after an onset of stimulation, oxidative phosphorylation in mitochondria must be in some way 'informed' about the current energy demand. Thus, energy supply can meet energy demand and the oxygen consumption flux and ATP turnover flux also increase greatly [3–8]. However, there is still no general agreement as to how oxidative phosphorylation is regulated during resting state → active state transition, that is which elements of the system are directly activated by some external effector and which are activated only indirectly, via changes in intermediate metabolite concentrations.

According to the classical (negative-feedback) mechanism, proposed originally by Chance and Williams on the basis of their studies on isolated mitochondria [9–11], only ATP usage is activated directly by an external effector (in this case, calcium ions), while oxidative phosphorylation and substrate dehydrogenation are activated only indirectly, via changes in [ADP], $[P_i]$ and $[NADH]/[NAD^+]$. Several authors [12–15] postulated that ATP usage and substrate dehydrogenation (e.g. irreversible TCA cycle dehydrogenases: pyruvate dehydrogenase; isocitrate dehydrogenase; and 2-oxoglutarate dehydrogenase) are directly activated in parallel by an external effector (calcium ions), while oxidative phosphorylation is activated only indirectly, via an increase in [ADP], $[P_i]$ and/or $[NADH]/[NAD^+]$.

The previously developed model of oxidative phosphorylation in isolated skeletal muscle mitochondria suggested that only a direct parallel activation of several (or even all) steps of this process can account for the behaviour of the system at higher work intensities [16,17]. However, this model did not take into account some elements and properties of the bioenergetic system in intact muscle important for the functioning of this system on the physiological level [18,19]. First of all, it did not include the creatine kinase system, creatine kinase (CK) plus phosphocreatine (PCr)/creatine (Cr) pair. This system is important for the regulation of oxidative phosphorylation, because its presence in intact muscle allows large changes in the concentration of inorganic phosphate, while $[P_i]$ is essentially constant in isolated mitochondria [20]. Therefore, it was theoretically possible that large changes in $[P_i]$, accompanying the changes in [ADP], could explain the existing experimental data within the negative-feedback-activation paradigm. In such a case, the theoretical predictions made with the aid of the model of oxidative phosphorylation in isolated mitochondria would be not valid in intact muscle. Additionally, this model did not cover proton production/consumption in the cytosol, it described fluxes in arbitrary units, involved a great (suspension of mitochondria) external volume/mitochondrial volume ratio and it took into account a lower adenine nucleotide pool than that present in intact muscle.

The proposition that many different steps of oxidative phosphorylation are activated in parallel [16,17] was mostly based on the fact that large relative changes in the oxygen consumption flux are accompanied by only very small relative changes in intermediate metabolite concentrations ([ADP], Δp, [NADH]) [3–8,21,22]. However, there are still trials been undertaken to explain the regulation of oxidative phosphorylation in muscle during varying energy demand in terms of the negative-feedback mechanism involving changes in [ADP] and/or $[P_i]$. Jeneson et al. [8] proposed that the dependence of mitochondrial oxidative phosphorylation on ADP concentration is of at least a second order and that this fact could entirely explain the much smaller relative changes in [ADP] than in the oxidative phosphorylation flux. However, the authors do not distin-

guish clearly between the oxygen consumption flux and ATP turnover flux, relative changes in these fluxes are not equivalent to each other due to proton leak. Therefore, the relevance of their explanation for the oxygen consumption flux remains uncertain.

The Saks' group developed computer models involving 'compartmentalised energy transfer' [23,24], based on the assumption of considerable metabolite (particularly ADP) concentration gradients due to diffusion limitations. The authors claim to demonstrate with the aid of their computer simulations that compartmentalised energy transfer is able to explain the very constant level of [ADP] observed in intact heart at very different flux intensities [25–27]. However, their theoretical results have in fact little to do with diffusion limitations and are mostly due to the very low concentration (a few micromoles) of inorganic phosphate in resting muscle and large relative variations (100 times or more) in $[P_i]$ during resting state → active state transition assumed by the authors. On the other hand, much greater resting $[P_i]$ values and much smaller relative variations in $[P_i]$ are usually reported in the literature [27] (also see the discussion in [28]). Additionally, the discussed model is not able to explain the stability of other metabolite concentrations, especially [NADH] [29]. Therefore, there still remains a question if more physiological variations in $[P_i]$ have any significant impact on the regulation of oxidative phosphorylation in vivo.

In the present paper we extended and modified the previous model of oxidative phosphorylation in isolated skeletal muscle mitochondria in order to involve the properties of oxidative phosphorylation in intact oxidative skeletal muscle. By oxidative muscle we understood mitochondria-rich type I and type IIA fibres, constituting most of e.g. human locomotory muscles [30–32]. We incorporated the CK system into the model, expressed fluxes in absolute units, took into account the proton production/consumption by creatine kinase and proton efflux/influx through the cellular membrane and introduced physiological adenine nucleotide pool as well as a cytosol/mitochondria volume characteristic of skeletal muscle. Thus, the previous model for isolated mitochondria was put into a more physiological context.

Subsequently, we studied in a theoretical way the regulation of oxidative phosphorylation in skeletal muscle during transition from resting state to active state. We obtained that the dependence of the ATP turnover flux on [ADP] is actually of, approximately, second order, as proposed by Jeneson et al. [8]. However, we observed in our simulations a near-first-order dependence of oxygen consumption on ADP concentration, the difference was due to the proton leak. Our simulations also indicated that physiological variations in $[P_i]$ have only a minor effect on the respiration rate. Therefore, we conclude that the negative feedback via [ADP] and/or $[P_i]$ cannot entirely account for the regulation of oxidative phosphorylation in vivo at higher work intensities.

2. Model

The computer dynamic model of oxidative phosphorylation in mammalian oxidative skeletal muscle used in the present study was developed by modifying the model of oxidative phosphorylation in isolated skeletal muscle mitochondria built previously [16,18]. That model comprised explicitly of the following steps: substrate dehydrogenation; complex I; complex III; complex IV (cytochrome oxidase); proton leak; ATP synthase; ATP/ADP carrier; phosphate carrier; ATP usage; and adenylate kinase. The dependencies of the reaction rates of particular steps on different metabolite concentrations were expressed as appropriate kinetic equations. Changes over time in particular metabolite concentrations were expressed in the form of a set of differential equations. This set was integrated numerically, with the aid of a computer.

The model used in the present study was developed by incorporating into the model for isolated mitochondria the following elements: absolute oxygen consumption fluxes; creatine kinase (CK) system; production/consumption of cytosolic protons by this system; and efflux/influx of protons (plus buffering of proton concentration in the cytosol). There were also some minor changes

introduced: a greater external (cytosolic) adenine nucleotide pool concentration; and a new value of the mitochondrial volume/external (in this case, cytosolic) volume ratio.

2.1. Oxygen consumption fluxes

In the version of the model for isolated mitochondria [16,18], respiration rates were expressed in arbitrary units. In the present article, oxygen consumption is expressed in mM min^{-1} in order to scale the fluxes in real units and to facilitate comparison of computer simulations with experimental results. The rate constants (or maximal velocities) of all reactions were therefore multiplied by an appropriate factor.

The oxygen consumption fluxes measured experimentally in different states in skeletal muscle, as well as the values accepted in the model, are presented in Table 1. In the resting state, the proton leak is responsible for over a half of the oxygen consumption, while the remaining respiration rate is due to the ATP turnover [33]. Therefore, the relative increase in the respiration rate during muscle exercise is never equal to the relative increase in ATP turnover, although these two features are sometimes confused. For example, a 10-fold increase in the respiration rate would be equivalent to a more than 20-fold increase in ATP turnover.

The maximal respiration rate is similar in isolated mitochondria, skinned fibres, muscle homogenate and intact muscle during PCr recovery after exercise (see discussion by Tonkonogi and Sahlin [34]). This suggests that the capacity for oxygen consumption in isolated mitochondria equals roughly the capacity for oxygen consumption in mitochondria in intact non-stimulated

Table 1
Respiration rates[a] in different states in mammalian skeletal muscle

State	Experimentally-measured respiration rate (mM min^{-1})	References	Respiration rate accepted in the model (mM min^{-1})
State 4 (inhibited ATP turnover, entire V_{O_2} due to proton leak	0.21	[33]	0.21
Resting state (approx. 60% of respiration due to proton leak, approx. 40% due to ATP turnover)	0.22–0.35	[5,21,33]	0.30
Maximal V_{O_2} in isolated mitochondria[b], skinned fibres, muscle homogenates and intact muscle during PCr recovery[c]	3.0–4.0	[34,35] [overviewed in [34]]	3.7
Maximal V_{O_2} in working muscle	8.5 15.5 6.3 16	[34] [36] [5] [37]	7–15

[a] 1 mM min^{-1} = 0.24 mmol × kg dry $mass^{-1}$ × min^{-1}.
[b] Recalculated for intact muscle taking into account mitochondria density [34].
[c] Recalculated from ATP production using the P/O ratio = 6.

muscle. Therefore, the state of maximal respiration rate in skinned fibres, muscle homogenate and intact muscle during PCr recovery can be regarded as an equivalent of state 3 in isolated mitochondria (in all these cases the respiration rate is mainly stimulated by a high ADP concentration). A comparison of the respiration rates in state 3 and 4 presented in Table 1 gives an *R*CR ratio (state 3 respiration/state 4 respiration) equal to approx. 15–20. This value is slightly greater than the maximal *R*CR ratio measured in isolated skeletal muscle mitochondria, which equals approximately 10 [38]. A plausible explanation of this discrepancy seems to be the possibility that the inner mitochondrial membrane is slightly damaged during mitochondria isolation (at least in some fraction of mitochondria) and, therefore, the (averaged) intensity of proton leak in isolated mitochondria is a little greater than in mitochondria in situ. Taking into account this phenomenon, the rate constant of proton leak was decreased in relation to the rate constants of other processes within the model.

One can also see from Table 1 that the maximal oxygen consumption in working muscle can be several times greater than the maximal capacity of oxidative phosphorylation in non-stimulated muscle (during PCr recovery after exercise). This apparent discrepancy can be easily explained by direct activation of mitochondria by some external (in relation to oxidative phosphorylation) intracellular factor, in parallel with the activation of ATP usage (actinomyosin-ATPase and Ca^{2+}-ATPase) by calcium ions during muscle exercise. On the other hand, the direct stimulation of oxidative phosphorylation can be switched off during PCr recovery after exercise (and is, of course, absent from isolated mitochondria, skinned fibres and muscle homogenates). Taking into account the assumed resting oxygen consumption rate (0.3 mM min^{-1}), one can easily calculate that the respiration rate increases approximately 20–50 times during resting state → maximal exercise transition. Within the model, the maximal oxygen consumption in working muscle was assumed to be equal to 7–15 mM min^{-1}.

Of course, a potential alternative explanation of the difference between the maximal respiration rate in isolated mitochondria and in intact muscle is that mitochondria are damaged during isolation. However, this would mean that mitochondria are also 'damaged' or inactivated in skinned fibres, muscle homogenate and intact muscle during PCr recovery, where similar maximal respiration rates as in isolated mitochondria are observed [34,35]. This seems very unlikely, especially in the case of intact muscle during recovery. Furthermore, inactivation of mitochondria upon isolation is not able to explain the main experimental evidence of parallel activation of different steps, namely the stability of metabolite concentration during large flux variations. On the other hand, the fluxes presented in Table 1 were measured in different experiments carried out in different laboratories. Therefore, only a semi-quantitative comparison of these fluxes seems to be justified.

Both the resting and maximal oxygen consumption rate per kg of body mass in mammals depends on the size of the animal [39]. The above-quoted fluxes refer mainly to medium-size mammals (humans, dogs and so on). References [21] and [33] concern rat muscle, but the resting respiration rate is similar in dog [5] and rat [21]. Moreover, those references were used mainly in order to assess the relative contribution of proton leak to the respiration rate in resting state.

2.2. Creatine kinase system

The main modification performed within the model was the introduction of the creatine kinase system: CK plus the creatine (Cr)/phosphocreatine (PCr) pair. The total creatine pool concentration $C_T = [Cr] + [PCr]$ was assumed to be equal to 35 mM [40,41]. The reaction catalysed by creatine kinase was assumed to be very close to thermodynamic equilibrium in skeletal muscle both in resting state and during intensive exercise. This assumption is based on both experimental studies [42,43] and theoretical quantitative considerations [40,44]. For example, the maximal ATP synthesis by creatine kinase is 11 times greater than the maximal ATP synthesis by oxidative phosphorylation [45]. Therefore, the CK system seems to fulfil two main functions in the muscle cell: (1) the PCr/Cr pair is the buffer for the ATP/ADP

ratio; and (2) the quick diffusion of Cr overcomes possible limitations in ADP diffusion [46]. For the above reasons, the diffusion limitations and displacement of CK from equilibrium assumed by Saks and co-workers in their models of oxidative phosphorylation in heart [23,24] were not taken into account in the present model. The cited authors developed their models in order to explain the very small variations in [ADP] observed in intact heart [25–27]. However, as it is discussed in the present article, the stability of [ADP] they obtained in their simulations was mostly due to unphysiologically large variations in $[P_i]$ assumed in their model and not due to compartmentalised energy transfer.

The apparent equilibrium constant of creatine kinase:

$$K_{obs} = K_{CK} \cdot H_e^+ = \frac{ATP_e \cdot Cr}{ADP_e \cdot PCr} \quad (1)$$

is equal to approximately 220 [47] in the conditions prevailing in resting muscle ($[Mg^{2+}] = 3$–4 mM [45], $pH_e = 7.0$). In fact, this equilibrium description would be completely sufficient to calculate the PCr/Cr ratio in all conditions on the basis of a current ATP/ADP ratio and pH. However, in order to involve explicitly the proton production/consumption by creatine kinase during transition between different steady-states, a fully equivalent kinetic description is used where the forward and backward reaction rates are described by a linear dependence on substrate concentrations (see Table 2). The greater the rate constants k_{fCK} and k_{bCK} (of course, their ratio has to fulfil the equilibrium requirements given by Eq. (1), the closer the reaction to thermodynamic equilibrium. Therefore, high enough values of these rate constants were chosen, ensuring that creatine kinase was near equilibrium in all conditions considered in the present paper (even at maximal ATP turnover fluxes). There is no need for a more complicated kinetic description of creatine kinase, especially so that the relevant kinetic parameters are difficult to measure and a great range of their values was obtained in different studies [46].

2.3. Proton efflux

The efflux of protons from cytosol to blood depends linearly on the cytosolic pH (pH_e) [48,49] and can be expressed by the following equation (see also Table 2):

$$v_{EFF} = k_{EFF}(pH_0 - pH_e) \quad (2)$$

where $pH_0 = 7.0$ and $k_{EFF} = 10$ mM min^{-1} [48,49]. Of course, when $pH_e > pH_0$ (e.g. after an onset of work, when protons are consumed by the CK-catalysed reaction), protons flow from outside to inside of muscle cells and we deal with an influx (negative efflux) of protons. Therefore, the flow of protons through the cellular membrane can be called the efflux/influx of protons.

2.4. Cytosolic proton buffering

The buffering of cytosolic proton concentration is described similarly as the buffering of protons in mitochondrial matrix [50]. The efficiency of buffering is expressed as follows:

$$r_{buffe} = c_{buffe}/c_{0e} \quad (3)$$

where $c_{buffe} = 0.025$ M H^+ per pH unit [48] is the cytosolic buffering capacity and c_{0e} stands for the 'natural' buffering capacity:

$$c_{0e} = (10^{-pH_e} - 10^{-pH_e - d\,pH})/d\,pH \quad (4)$$

where dpH is a small change in pH_e. R_{buff} appears in the differential equation describing the balance of the reactions producing and consuming cytosolic protons (see Table 2).

2.5. Other changes

The concentration of the external (cytosolic) adenine nucleotide pool $A_T = [ATP] + [ADP] + [AMP]$ was increased to 6.7 mM in order to reflect the situation prevailing in intact muscle cells [35,40,43,45,51]. The concentration of the total cytosolic phosphate pool $P_T = [PCr] + 3[ATP] + 2[ADP] + [AMP] + [P_i]$ equal to approximately 48 mM was accepted [40] (however, be-

Table 2
Concise complete kinetic description of the dynamic model of oxidative phosphorylation in intact skeletal muscle

Kinetic equations
(All reaction rates are expressed in $\mu M\ min^{-1}$).
Substrate dehydrogenation:

$$v_{DH} = k_{DH} \frac{1}{\left(1 + \frac{K_{mN}}{NAD^+/NADH}\right)^{P_D}}$$

$k_{DH} = 28\,074\ \mu M\ min^{-1}$, $K_{mN} = 100$, $p_D = 0.8$.

Complex I:

$$v_{C1} = k_{C1} \Delta E_{C1}$$

$k_{C1} = 238.95\ \mu M\ mV^{-1}\ min^{-1}$

Complex III:

$$v_{C3} = k_{C3} \Delta E_{C3}$$

$k_{C3} = 136.41\ \mu M\ mV^{-1}\ min^{-1}$

Complex IV:

$$v_{C4} = k_{C4} \cdot a^{2+} \cdot c^{2+} \frac{1}{1 + \frac{K_{mO}}{O_2}}$$

$k_{C4} = 3.60\ \mu M^{-1}\ min^{-1}$, $K_{mO} = 120\ \mu M$ (apparent $K_{mO} = 0.8\ \mu M$)

ATP synthase:

$$v_{SN} = k_{SN} \frac{\gamma - 1}{\gamma + 1}$$

$k_{SN} = 34\,316\ \mu M\ min^{-1}$, $\gamma = 10^{\Delta G_{SN}/Z}$

ATP/ADP carrier:

$$v_{EX} = k_{EX} \cdot \left(\frac{ADP_{fe}}{ADP_{fe} + ATP_{fe} \cdot 10^{-\psi_i/Z}} - \frac{ADP_{fi}}{ADP_{fi} + ATP_{fi} \cdot 10^{-\psi_i/Z}} \right) \cdot \left(\frac{1}{1 + K_{mADP}/ADP_{fe}} \right)$$

$k_{EX} = 54\,572\ \mu M\ min^{-1}$, $K_{mADP} = 3.5\ \mu M$

Phosphate carrier:

$$v_{PI} = k_{PI} \cdot (Pi_{je} \cdot H_e - Pi_{ji} \cdot H_i)$$

$k_{PI} = 69.421\ \mu M^{-1}\ min^{-1}$

ATP usage:

$$v_{UT} = k_{UT} \frac{1}{1 + \frac{K_{mA}}{ATP_{te}}}$$

$k_{UT} = 686.50\ \mu M\ min^{-1}$ (resting state), $K_{mA} = 150\ \mu M$

Proton leak:

$$v_{LK} = k_{LK1} \cdot (e^{k_{LK2} \cdot \Delta p} - 1)$$

$k_{LK1} = 2.500\ \mu M\ min^{-1}$, $k_{LK2} = 0.038\ mV^{-1}$

Adenylate kinase:

$$v_{AK} = k_{AK} \cdot ADP_{fe} \cdot ADP_{me} - k_{bAK} \cdot ATP_{me} \cdot AMP_e$$

$k_{fAK} = 862.10\ \mu M^{-1}\ min^{-1}$, $k_{bAK} = 22.747\ \mu M^{-1}\ min^{-1}$

Table 2 (*Continued*)

Creatine kinase:

$v_{CK} = k_{fCK} \cdot ADP_{te} \cdot PCr \cdot H_e^{+} - k_{bCK} \cdot ATP_{te} \cdot Cr$

$k_{fCK} = 1.9258\ \mu M^{-2}\ min^{-1}$, $k_{bCK} = 0.00087538\ \mu M^{-1}\ min^{-1}$

Proton efflux:

$v_{EFF} = k_{EFF} \cdot (pH_0 - pH_e)$

$k_{EFF} = 10\,000\ \mu M\ min^{-1}$, $pH_0 = 7.0$

Set of differential equations

$\dot{NADH} = (v_{DH} - v_{C1}) \cdot R_{cm}/B_N$

$\dot{UQH}_2 = (v_{C1} - v_{C3}) \cdot R_{cm}$

$\dot{c}^{2+} = (v_{C3} - 2 \cdot v_{C4}) \cdot 2 \cdot R_{cm}$

$\dot{O}_2 = 0$ (constant saturated oxygen concentration = 240 μM) or $\dot{O}_2 = -v_{C4}$

$\dot{H}_e^{+} = -(2 \cdot (2 + 2 \cdot u) \cdot v_{C4} + (4 - 2 \cdot u) \cdot v_{C3} + 4 \cdot v_{C1} - n_A \cdot v_{SN} - u \cdot v_{EX} - (1 - u) \cdot v_{PI} - v_{LK}) \cdot R_{cm}/r_{buffi}$

$\dot{ATP}_{ti} = (v_{SN} - v_{EX}) \cdot R_{cm}$

$\dot{P}i_{ti} = (v_{PI} - v_{SN}) \cdot R_{cm}$

$\dot{ATP}_{te} = v_{EX} - v_{UT} + v_{AK} + v_{CK}$

$\dot{ADP}_{te} = v_{UT} - v_{EX} - 2 \cdot v_{AK} - v_{CK}$

$\dot{P}i_{te} = v_{UT} - v_{PI}$

$\dot{PCr} = -v_{CK}$

$\dot{H}_e^{+} = (2 \cdot (2 + 2 \cdot u) \cdot v_{C4} + (4 - 2 \cdot u) \cdot v_{C3} + 4 \cdot v_{C1} - n_A \cdot v_{SN} - u \cdot v_{EX} - (1 - u) \cdot v_{PI} - v_{LK} - v_{CK} - v_{EFF})/r_{buffe}$

$R_{cm} = 15$ (cell volume/mitochondria volume ratio)

$B_N = 5$ (buffering capacity coefficient for NAD)

Calculations

$c^{3+} = c_t - c^{2+}$

$c_t = 270\ \mu M$, ($= c^{2+} + c^{3+}$, total concentration of cytochrome c)

$UQ = U_t - UQH_2$

$U_t = 1350\ \mu M$, ($= UQH_2 + UQ$, total concentration of ubiquinone)

$NAD^{+} = N_t - NADH$

$N_t = 2970\ \mu M$, ($= NADH + NAD^{+}$, total concentration of NAD)

$AMP_e = A_{eSUM} - ATP_{te} - ADP_{te}$

$A_{eSUM} = 6700.2\ \mu M$, ($= ATP_{te} + ADP_{te} + AMP_e$, total external adenine nucleotide concentration)

$ADP_{ti} = A_{iSUM} - ATP_{ti}$

$A_{iSUM} = 16\,260\ \mu M$, ($= ATP_{ti} + ADP_{ti}$, total internal adenine nucleotide concentration)

Table 2 (*Continued*)

$Cr = C_{SUM} - PCr$
$C_{SUM} = 35\,000$ μM, (= Cr + PCr, total creatine concentration)

$P_{SUM} = 55\,659$ μM (= PCr + $3ATP_{te} + 2ADP_{te} + AMP_e + Pi_{te} + (3ATP_{ti} + 2ADP_{ti} + Pi_{ti})/R_{cm}$, total phosphate pool)
$Mg_{fe} = 4000$ μM, (free external magnesium concentration)

$ATP_{fe} = ATP_{te}/(1 + Mg_{fe}/k_{DTe})$
$k_{DTe} = 24$ μM, (magnesium dissociation constant for external ATP)

$ATP_{me} = ATP_{te} - ATP_{fe}$

$ADP_{fe} = ADP_{te}/(1 + Mg_{fe}/k_{DDe})$
$k_{DDe} = 347$ μM, (magnesium dissociation constant for external ADP)

$ADP_{me} = ADP_{te} - ADP_{fe}$
$Mg_{fi} = 380$ μM, (free internal magnesium concentration)

$ATP_{fi} = ATP_{ti}/(1 + Mg_{fi}/k_{DTi})$
$k_{DTi} = 17$ μM, (magnesium dissociation constant for internal ATP)

$ATP_{mi} = ATP_{ti} - ATP_{fi}$

$ADP_{fi} = ADP_{ti}/(1 + Mg_{fi}/k_{DDi})$
$k_{DDi} = 282$ μM, (magnesium dissociation constant for internal ADP)

$ADP_{mi} = ADP_{ti} - ADP_{fi}$
$T = 289$K
$R = 0.0083\ \text{kJ} \times \text{mol}^{-1} \times \text{K}^{-1}$
$F = 0.0965\ \text{kJ} \times \text{mol}^{-1} \times \text{mV}^{-1}$
$S = 2.303 \times R \times T$
$Z = 2.303 \times R \times T/F$
$u = 0.861$, (= Δψ/Δp)

$pH_e = -\log(He/1\,000\,000)$ (He expressed in μM)
$pH_i = -\log(H_i/1\,000\,000)$ (H_i expressed in μM)
$\Delta pH = Z\ (pH_i - pH_e)$
$\Delta p = 1/(1 - u)\ \Delta pH$
$\Delta\psi = -(\Delta p - \Delta pH)$
$\psi i = 0.65 \times \Delta\psi$
$\psi e = -0.35 \times \Delta\psi$
$c_{0i} = (10^{-pHi} - 10^{-pHi-dpH})/d\text{pH}$, ('natural' buffering capacity for H^+ in matrix), $d\text{pH} = 0.001$
$r_{buffi} = c_{buffi}/c_{0i}$, buffering capacity coefficient for H^+ in matrix)
$c_{buffi} = 0.022$ M H^+/pH unit, (buffering capacity for H^+ in matrix)
$c_{0e} = (10^{-pHe} - 10^{-pHe-dpH})/d\text{pH}$, ('natural' buffering capacity for H^+ in cytosol), $d\text{pH} = 0.001$
$r_{buffe} = c_{buffe}/c_{0e}$, buffering capacity coefficient for H^+ in cytosol)
$c_{buffe} = 0.025$ M H^+/pH unit, (buffering capacity for H^+ in cytosol)
$Pi_{je} = Pi_{te}/(1 + 10^{pHe-pKa})$
$Pi_{ji} = Pi_{ti}/(1 + 10^{pHi-pKa})$
$pK_a = 6.8$
$\Delta G_{SN} = n_A \times \Delta p - \Delta G_P$, (thermodynamic span of ATP synthase)
$\Delta G_P = \Delta G_{P0}/F + Z \times \log(1\,000\,000 \times ATP_{ti}/(ADP_{ti} \times Pi_{ti}))$ (concentrations expressed in μM)
$n_A = 2.5$, (phenomenological H^+/ATP stoichiometry of ATP synthase)
$\Delta G_{P0} = 31.9\ \text{kJ} \times \text{mol}^{-1}$

Table 2 (*Continued*)

$E_{mN} = E_{mN0} + Z/2 \times \log(NAD^+/NADH)$, (NAD redox potential)
$E_{mN0} = -320$ mV
$E_{mU} = E_{mU0} + Z/2 \times \log(UQ/UQH_2)$, (ubiquinone redox potential)
$E_{mU0} = 85$ mV
$E_{mc} = E_{mc0} + Z \times \log(c^{3+}/c^{2+})$, (cytochrome c redox potential)
$E_{mc0} = 250$ mV
$E_{ma} = E_{mc} + \Delta p \times (2 + 2u)/2$, (cytochrome a_3 redox potential)
$A_{3/2} = 10^{(Ema - Ema0)/Z}$, ($a^{3+}/a^{2+}$ ratio)
$a^{2+} = a_t/(1 + A_{3/2})$, (concentration of reduced cytochrome a_3)
$a^{3+} = a_t - a^{2+}$
$a_t = 135$ μM
$E_{ma0} = 540$ mV
$\Delta G_{C1} = E_{mU} - E_{mN} - \Delta p \times 4/2$, (thermodynamic span of complex I)
$\Delta G_{C3} = E_{mc} - E_{mU} - \Delta p \times (4 - 2u)/2$, (thermodynamic span of complex III)

Subscripts: e, external (cytosolic); i, internal (mitochondrial); t, total; f, free; m, magnesium complex; j, monovalent.

cause inorganic phosphate can be exchanged between the cytosolic pool and mitochondrial pool, the total phosphate pool constitutes a real constant parameter, see Table 2). The ratio of the cytosol volume to the mitochondrial matrix volume (R_{cm}) was assumed to be equal to 15. Thus, it was accepted that mitochondria occupies approximately 7% of the myocyte volume [52,53].

2.6. Glycolysis

Glycolytic production of ATP and of protons was not incorporated into the model. It is so that oxidative phosphorylation is the main energy production system in oxidative skeletal muscle under most conditions (even in hypoxia) and in most human physical activities [3,35,54–56], although undoubtedly glycolysis plays an important role during short-term maximal exercise. Additionally, quantitative kinetic data concerning glycolysis in skeletal muscle seem to be insufficient to work out a satisfactory mathematical description of this process. No detailed quantitative model of glycolysis in skeletal muscle has been worked out, while models of this process in other tissues cannot be easily and reliably incorporated into the model of oxidative phosphorylation in muscle, especially that it is not certain how glycolysis is activated, by changes in intermediate metabolite concentrations or by direct activation of different enzymes. Furthermore, the present article deals mainly with oxygen consumption fluxes and not with ATP turnover fluxes. In order to check very roughly the effect of glycolytic ATP supply on the relation between oxygen consumption and [ADP], we introduced to our model several very simple kinetic descriptions of glycolysis, e.g. a linear dependence of this process on [AMP] and/or [ADP] (the most important activators of glycolysis). Then, we tested the influence of the additional ATP production on the system properties. The general, semi-quantitative effect was the same in all the cases checked, at a given particular energy demand, the additional glycolytic ATP production decreased oxygen consumption and increased the [ATP]/[ADP] ratio [data not shown]. However, what is most important is that the relationship between the respiration rate and phosphorylation potential remained completely unchanged (in fact, this is what should be expected intuitively, because the kinetic dependence of oxidative phosphorylation on the 'components' of the phosphorylation potential is the same in the presence of glycolysis; the latter process can only affect mitochondrial ATP production via [ADP], [P_i] and

[ATP]). Therefore, we concluded that glycolysis had essentially no impact on the relationship between the oxygen consumption flux and the concentrations of ADP, P_i and ATP which we studied in the present article.

Nevertheless, the omission of glycolysis is certainly an approximation and one should bear in mind that e.g. the increase in pH_e after the onset of contraction is most probably overestimated in computer simulations due to the lack of the glycolytic proton production. On the other hand, theoretical predictions of the model agree fairly well with the experimental data suggesting that proton influx/efflux counteract effectively large changes in cytosolic pH as a result of proton production/consumption by CK-catalysed reaction (at least at low and moderate work intensities). However, glycolysis could be easily incorporated into the model, when only a simple quantitative kinetic description of this process in skeletal muscle becomes available and the details of its regulation are known.

A concise complete description of the model of oxidative phosphorylation in intact skeletal muscle used in the present study is given in the Table 2.

3. Theoretical results and discussion

First, the behaviour of the oxidative phosphorylation system in skeletal muscle for the negative-feedback mechanism, where only ATP usage is directly activated, while oxidative phosphorylation is activated indirectly, via changes in [ADP] and [P_i], was modelled. Fig. 1 represents the simulated dependence of the respiration rate and different metabolite concentrations on a relative energy

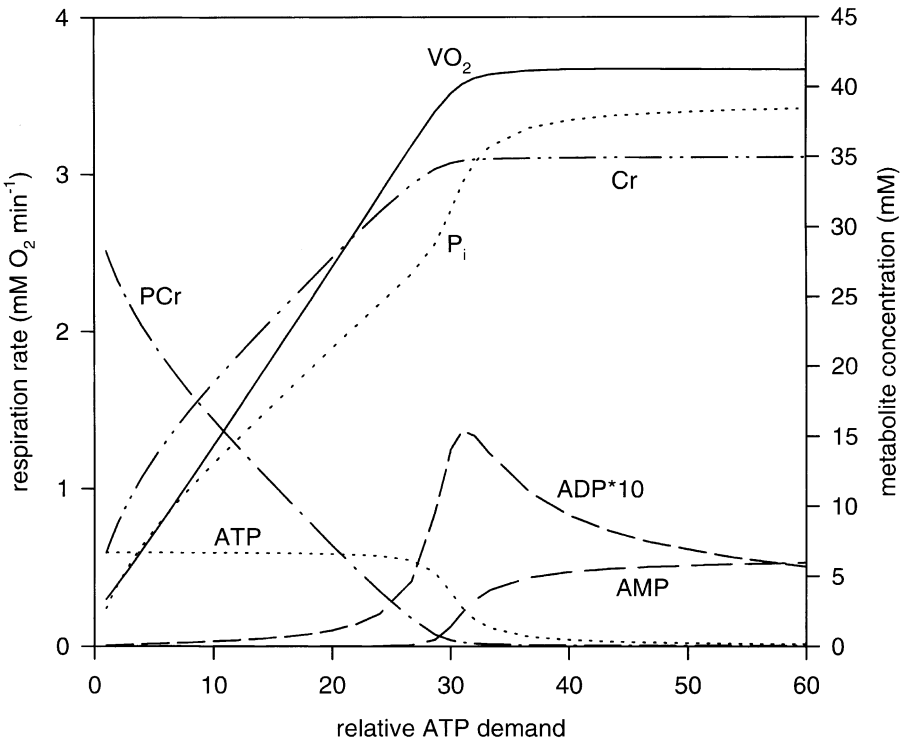

Fig. 1. Simulated dependence of the respiration rate and different metabolite concentrations on a relative energy demand in the case of negative-feedback mechanism. Energy demand corresponds to the current rate constant of ATP usage and is standardised to equal to 1 in the resting state.

demand. Within the model, energy demand was equivalent to the current rate constant of ATP usage (k_{UT}) in a given state (see Table 2). In Fig. 1, this rate constant was standardised to equal to 1 in the resting state. Then the energy demand was gradually increased and the simulated values of fluxes and metabolite concentrations in subsequent steady-states were recorded.

It can be seen that the respiration rate increases linearly with an increase in ATP demand until the demand reaches approximately 30 (a 30-fold increase in relation to resting state). Then oxygen consumption stabilises at approximately 3.7 mM min^{-1}. This is an equivalent of state 3 in isolated mitochondria. The concentrations of PCr and Cr change in a near-linear manner until state 3 is reached and afterwards they remain constant ([PCr] approaches zero while [Cr] approaches C_T]). Initially, the inorganic phosphate concentration also increases linearly, in the vicinity of state 3 the increase becomes steeper and then terminates, [P_i] does not change any more. [ATP] remains essentially constant before state 3 is reached and then decreases sharply to a very low value. The concentration of ADP increases quickly with accelerating speed during transition from resting state to state 3 (generally, an approx. 200-fold increase takes place) and then decreases a little due to the adenylate kinase equilibrium. [AMP] is very low between resting state and state 3 and increases greatly when state 3 is reached. However, [ATP] and [ADP] do not ultimately fall to zero and [AMP] does not reach A_T because in state 3 the concentration of ATP approaches the Michaelis–Menten constant of ATP usage for ATP and therefore, a further increase in the maximal velocity of ATP usage cannot effectively affect the system.

Fig. 2 presents the simulated relationship between [ADP] and respiration rate, extracted from the data shown in Fig. 1 (solid line in Fig. 2). This near-hyperbolic relationship constitutes only apparent dependence because respiration rate is stimulated not only by an increase in [ADP] but also by an increase in inorganic phosphate concentration. In intact muscle, [P_i] can change significantly due to the presence of the CK system (CK + PCr/Cr pair), which is not the case in

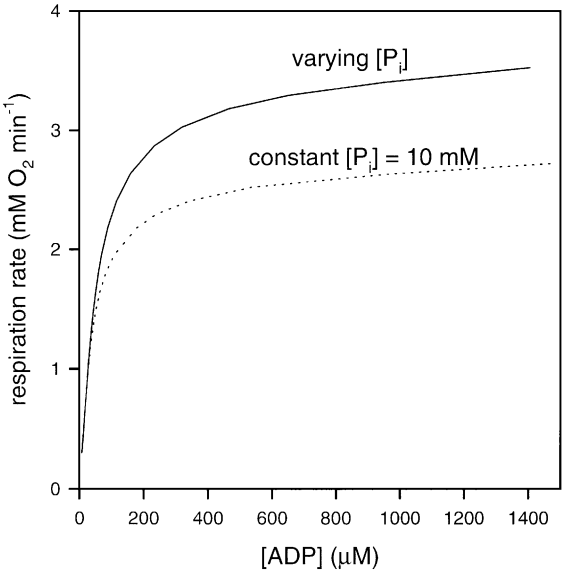

Fig. 2. Simulated relationship between [ADP] and the respiration rate for a varying (thanks to the existence of the CK system) [P_i] (solid line) and for a fixed [P_i] equal to 10 mM (situation analogous to that prevailing in isolated mitochondria) (dotted line).

isolated mitochondria, where [P_i] remains essentially constant. Therefore, in order to study the effect of CK system on the behaviour of oxidative phosphorylation, a simulation analogous to the one presented in Fig. 1, but with a constant fixed [P_i] = 10 mM (a concentration frequently applied in the isolated mitochondria system) was performed. The dotted line in Fig. 2 represents the simulated relation between [ADP] and respiration rate in this situation. It can be seen that a varying [P_i] (accompanying a varying [ADP]) is able to stimulate oxygen consumption by up to 30% more than a varying [ADP] alone does. The difference is quite significant but the ADP concentration still remains the main factor affecting the respiration rate, especially at lower (physiological) ADP levels. Therefore, [ADP] can be regarded as a predominating regulatory factor that determines the rate of oxygen consumption (and ATP turnover) in skeletal muscle in the case of the negative-feedback mechanism.

This conclusion is particularly important in the light of the models of oxidative phosphorylation

in working heart developed recently by Saks and co-workers [23,24]. The authors claim that they are able, assuming 'compartmentalised energy transfer', to explain the essentially constant ADP concentration at very different oxygen consumption fluxes [25–27], without the necessity to refer to the direct activation of (different steps of) oxidative phosphorylation, or even of substrate dehydrogenation. Unfortunately, their simulations remain in contradiction with several experimental results. These simulations suggest explicitly that the PCr/ATP ratio decreases two times during a five-fold increase in the flux (fig. 14b in [23]), while essentially no changes in this ratio were observed in experiments [27,57]. In fact, the stability of [ADP] obtained in the cited articles has little to do with the postulated compartmentalised energy transfer, and is based on the assumption that P_i concentration is very low (a few μM) in a slowly-beating heart, and therefore, it limits the flux, while this concentration increases dramatically (to 12000 μM, by 3–4 orders of magnitude) during activation of heart work (fig. 14d in [23]). This assumption stands in severe conflict with many experimental results, where relatively small (approx. 50–100%) or no changes in $[P_i]$ are reported at all, while the (measured or estimated) inorganic phosphate concentration in slowly-beating heart is, roughly, between 500 and 2000 μM (e.g. [27], see also the discussion in [28]). Also the extended version of this model [24] predicts huge relative changes in $[P_i]$ (see fig. 9 in [24]). Additionally, the discussed model cannot explain the relatively constant $NADH/NAD^+$ ratio in heart [29]. On the other hand, our present model, which takes into account physiological changes in inorganic phosphate concentration, leads to the conclusion that P_i does not constitute an important factor regulating oxidative phosphorylation in intact muscle. Therefore, we conclude that the regulation of oxidative phosphorylation by the negative-feedback mechanisms involving changes in [ADP] and/or $[P_i]$ cannot alone account for the behaviour of the system in vivo. The theoretical results concerning the stability of [ADP] obtained by Saks and co-workers can be mimicked within our model, which does not take into account any diffusion limitations, when the resting state is assumed to be very close to state 4 (data not shown). In such a case, the concentra-

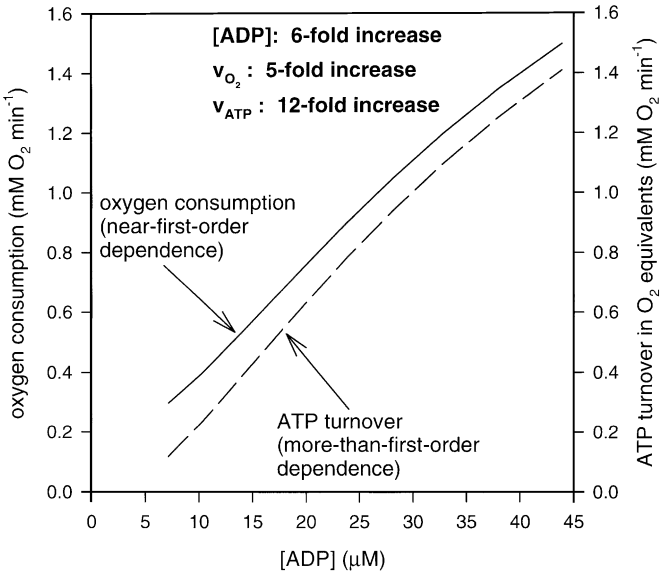

Fig. 3. Simulated relationship between the oxygen consumption flux, ATP turnover flux and [ADP] at low ADP concentrations. ATP turnover flux is expressed in O_2 equivalents, in order to enable an easy comparison with the overall oxygen consumption flux (corresponding to both ATP turnover and proton leak).

tion of inorganic phosphate equals a few μM, and ATP turnover can be increased significantly by an increase in $[P_i]$, without significant changes in [ADP]. However, in this situation the proton leak accounts for almost 100% of the respiration rate and phosphate concentration is extremely low, which contradicts experimental results [33,28].

Fig. 3 shows the simulated dependence of the oxygen consumption flux and ATP turnover flux on [ADP] (at varying $[P_i]$) at low ADP concentrations. As it is expected, the relationship between respiration rate and [ADP] is here near-proportional (a near-first-order reaction), a five-fold increase in the respiration rate accompanies a six-fold increase in [ADP]. On the other hand, ATP turnover depends much more steeply on the ADP concentration, a six-fold increase in [ADP] causes a 12-fold increase in ATP turnover. The reaction order approaches 2 in this case. This is caused by complex kinetics of the ATP/ADP carrier presented in Table 2. Such a dependence was observed in experimental studies on an isolated ATP/ADP carrier [58]. The difference in the kinetics (order) of the oxygen consumption flux and ATP turnover flux is, of course, due to the proton leak, which corresponds to at least one half of oxygen consumption in resting muscle [33]. This causes relative changes in the respiration rate to be at least twice smaller than the relative changes in ATP turnover.

Jeneson and co-workers [8] have proposed that the above-discussed phenomenon alone should explain the steep dependence of ATP turnover on [ADP] in skeletal muscle. They drew attention to the fact that a near-second-order dependence between ADP concentration and ATP turnover (and, in a few cases, oxygen consumption) flux was observed in isolated mitochondria and proposed that this fact alone could explain the results they had obtained in intact muscle (over 20-fold increase in ATP turnover vs. approx. four-fold increase in [ADP]). However, computer simulations performed by means of the model developed in the present paper do not confirm this proposition. Furthermore, the kinetics of oxygen consumption flux, which is predominantly dealt with in the present article, is still near-hyperbolic (near-first-order at low ADP concentrations). In most experiments, a near-hyperbolic (near-first-order at low ADP concentrations) dependence of the respiration rate on [ADP] is observed. The more than 20-fold increase in ATP turnover observed [8] corresponds approximately to a 10-fold increase in oxygen consumption (assuming that approx. 60% of resting-state respiration is due to proton leak), while only a 3.3-fold increase in the respiration rate can be caused by the measured four-fold increase in [ADP] [8] (see Fig. 3). In conclusion, the near-second-order dependence on [ADP] refers only to the ATP-turnover flux, but not to the oxygen-consumption flux (the difference being due to proton leak).

Additionally, the authors estimated the ATP turnover flux from the initial rate of a decrease in [PCr]. However, this estimation is only valid in the case of the negative-feedback mechanism. On the other hand, if ATP (and PCr) production and consumption are activated in parallel, the actual ATP turnover can be essentially greater than the initial rate of PCr depletion. This would lead to a substantial underestimation of the (relative changes in) ATP turnover flux.

The simulated dependence between [ADP] and respiration rate for the case of the negative-feedback mechanism (Fig. 3) is in good agreement with several experimental data obtained for low work intensities in skeletal muscle under electrical stimulation, where a near-first-order or near-hyperbolic kinetics of oxygen consumption were observed [57,59,60]. Therefore, the negative feedback activation via [ADP] can be the main mechanism regulating oxidative phosphorylation under these conditions. However, this mechanism is not able to explain the changes in the respiration rate and [ADP] taking place in skeletal muscle during transition from rest to high work intensities [3–8]. Additionally, even some experimental data for low work intensities cannot be explained within the negative-feedback paradigm. For example, the protonmotive force (Δp) does not change, or even slightly increases, during a two-fold stimulation of oxygen consumption in muscle [21]. This experimental result is supported by the effect of calcium ions on isolated skeletal muscle

mitochondria, where an increase in the respiration rate is accompanied by essentially no changes in the protonmotive force [61].

Fig. 4 represents simulated time-courses of [PCr], [P_i] and cytosolic pH during stimulation of muscle and recovery for three different (but relatively low) increases in energy demand in the case of negative-feedback mechanism. The concentrations of PCr and inorganic phosphate change in a near-exponential way — similar behaviour was observed in experimental studies [41,60]. The simulated relationship between [PCr] and ATP turnover, presented in Fig. 5, is near-linear which is also in agreement with experimental results [41,60]. The overshoot of [PCr] observed sometimes during recovery [60], which does not appear in the above simulations, can be explained by the fact that the direct activation of the oxidative phosphorylation system and/or substrate dehydrogenation is not completely switched off immediately after the end of work and onset of recovery, but a little later. Nevertheless, generally, also in this case, experimental results can be fairly well explained within the paradigm of the negative-feedback mechanism. However, these experiments were performed using electrical stimulation of muscle and relatively low increases in work intensity above its resting-state value. Additionally, relative changes in the respiration rate were not measured in the discussed experiments, and therefore it is possible that also in this case a direct activation of substrate dehydrogenation and oxidative phosphorylation is necessary to explain the behaviour of the system.

The simulated changes in cytosolic pH after stimulation and during recovery (up to approx. 0.2 units) are a little greater than those observed in experiments [35,51] (although even higher changes are observed in some experiments at higher work intensities [49]). This is probably due to the fact that glycolytic proton production is not included in the model. However, generally, the simulated changes in pH_e are relatively small, which can suggest that proton efflux/influx alone can effectively counteract large changes in cytosolic proton concentration (at least at low and moderate work intensities).

The arguments supporting the idea of a direct activation of several (all) steps of oxidative phosphorylation in parallel with activation of ATP

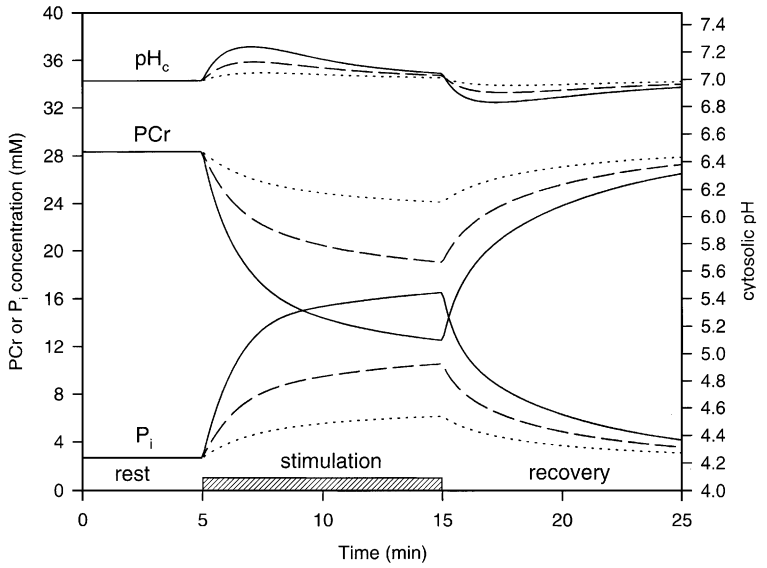

Fig. 4. Simulated time courses of the concentration of PCr and P_i as well as of cytosolic pH after an onset of muscle stimulation and during recovery for three stimulation intensities (increases in energy demand): 3.5 fold (dotted line); eight fold (dashed line); and 15 fold (solid line).

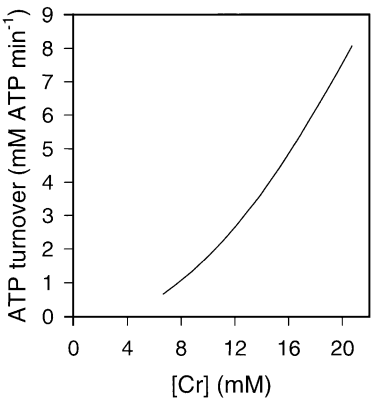

Fig. 5. Simulated relationship between [Cr] and ATP turnover rate extracted from the data presented in Fig. 4.

usage and substrate dehydrogenation are discussed in more detail elsewhere [16,17]. To add one more example, we modelled one particular set of experimental data obtained by Hogan and co-workers for electrically-stimulated dog gastrocnemius [5] in order to determine what activation of ATP-consumption and ATP-production could be expected in that case. The theoretical results obtained are presented in Fig. 6. Experimental points for resting state, sub-maximal and maximal work are compared with a line joining simulated points. For each state, the degrees of activation of ATP-production and ATP consumption used in simulations are indicated (of course, in resting state both sub-systems are activated once, that is they are not activated). It can be seen that a large (five–eight-fold) direct activation of the substrate dehydrogenation + oxidative phosphorylation sub-system is necessary to account for the reported changes in the respiration rate and [ADP]. At the same time no combination of a direct activation of only ATP usage and substrate dehydrogenation was able to produce the expected changes in oxygen consumption and ADP concentration. It must be emphasised that our present model takes into account both physiological changes in $[P_i]$ and the near-second-order dependence of ATP synthesis on [ADP] discussed above. Nevertheless, they are not able alone to account entirely for the behaviour of the system in vivo. Therefore, a direct activation of the oxidative phosphorylation block was necessary to explain the analysed experimental results.

When analysing the experimental data concerning intact skeletal muscle, it must be taken into account that this tissue is heterogeneous with regard to fibre types and activation of fibres. It seems to be the case that there is a hierarchy of recruitment of different muscle fibres during increasing work intensity. Therefore, relative changes of [ADP] in individual working fibres can be underestimated when the average concentration in an entire muscle is measured experimentally. However, in such a case, relative changes in oxygen consumption by individual working fibres would also be underestimated. Therefore, the ratio of the relative change in oxygen consumption to the relative change in ADP would remain approximately the same. It should be also stressed that the idea of parallel activation is supported not only by the stability of ADP concentration, but also by constancy of [NADH] and Δp during resting state → active state transition [21,22].

To sum up, the modifications of the previous model for isolated mitochondria (addition of the CK system, greater adenine nucleotide pool, smaller external volume/mitochondria volume

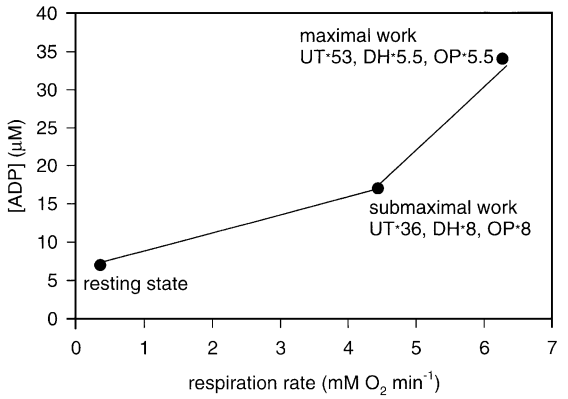

Fig. 6. Simulation of the relationship between [ADP] and respiration rate obtained experimentally by Hogan and co-workers in dog gastrocnemius during transition from resting state to sub-maximal and maximal work [5]. Experimental data (points), simulated dependence (line) as well as the degree of activation of ATP utilisation (UT), substrate dehydrogenation (DH) and oxidative phosphorylation (OP) used in simulations are presented.

ratio) did not significantly affect the properties of the oxidative phosphorylation system. Therefore, the performed simulations suggest that general properties of this system are similar in isolated mitochondria and in intact muscle. The computer model of oxidative phosphorylation in mammalian oxidative skeletal muscle developed in the present study seems to be a useful tool in theoretical studies on the regulation of this process during resting state → active state transition. It shows that physiological changes in $[P_i]$ do not affect significantly the kinetic properties of oxidative phosphorylation and that the near-second-order dependence on [ADP] concerns only the ATP synthesis flux and not the oxygen consumption flux. Consequently, the model predicts (in accordance with previous theoretical results obtained by means of the model of oxidative phosphorylation in isolated mitochondria) that some (not yet identified) cytosolic factor activates in parallel several components of the bioenergetic system in skeletal muscle (especially, at least some, and possibly all, oxidative phosphorylation complexes) during transition from resting state to intensive (sub-maximal or maximal) exercise caused by physiological neural stimulation. Therefore, it can produce testable predictions concerning the existence of some yet undiscovered phenomena, these predictions can be verified or falsified experimentally in the future. We plan to use this model for further theoretical studies.

Acknowledgements

This work was supported by the Polish State Committee for Scientific Research (KBN) grant number 4PO5D 05817.

Appendix A

Table 2 presents a concise complete description of the computer model of oxidative phosphorylation used in the present study. It contains kinetic equations, parameter values and rate constants which allow the calculation of fluxes and metabolite concentrations in different steady-states.

Different levels of energy demand (used in the simulations presented in Fig. 1–Fig. 5, concerning the negative-feedback mechanism) were established by fixing different values of the rate constant of ATP usage (k_{UT}). The value of this constant was 0 in state 4, 685.5 $\mu M\ min^{-1}$ in resting state and a certain multiplicity of this resting state value (indicated as relative energy demand in Fig. 1) in active states. In simulations concerning the mechanism involving parallel direct activation of different steps (Fig. 6), the rate constants of all oxidative phosphorylation complexes (complex I, complex III, complex IV, ATP synthase, ATP/ADP carrier, phosphate carrier) and substrate dehydrogenation were multiplied by some determined factor (indicated in Fig. 6), identical for each complex.

References

[1] P. Mitchell, Nature 191 (1961) 144–148.
[2] Mitchell, P. Chemiosmotic coupling and energy transduction, Glynn Research, Bodmin. 1968
[3] P.W. Hochachka, Muscles as Molecular and Metabolic Machines, CRC Press, Boca Raton, 1994.
[4] R.J. Rose, D.R. Hodgson, T.B. Kelso et al., J. App. Physiol. 64 (1988) 781–788.
[5] M.C. Hogan, P.G. Arthur, D.E. Bebout, P.W. Hochachka, P.D. Wagner, J. Appl. Physiol. 73 (1992) 728–736.
[6] G.P. Dobson, W.S. Parkhouse, J.M. Weber et al., Am. J. Physiol. 255 (1988) R513–R519.
[7] B.J. Clark, M.A. Acker, K. McCully et al., Am. J. Physiol. 254 (1988) C258–C266.
[8] J.A.L. Jeneson, R.W. Wiseman, H.V. Westerhoff, M.J. Kushmerick, J. Bioch. Chem. 271 (1996) 27995–27998.
[9] B. Chance, G.R. Williams, J. Biol. Chem. 217 (1955) 383–393.
[10] B. Chance, G.R. Williams, Adv. Enzymol. 17 (1956) 65–134.
[11] B. Chance, S. Eleff, J.S. Leigh, D. Sokolow, A. Sapega, Proc. Natl. Acad. Sci. USA 78 (1981) 6714–6718.
[12] R.M. Denton, J.G. McCormack, FEBS Lett. 119 (1980) 1–8.
[13] R.G. Hansford, Curr. Top. Bioenerg. 10 (1980) 217–278.
[14] J.G McCormack, A.P. Halestrap, R.M. Denton, Physiol. Rev. 70 (1990) 391–425.
[15] J.G. McCormack, R.M. Denton, Biochim. Biophys. Acta 1018 (1990) 278–291.
[16] B. Korzeniewski, Biochem. J. 330 (1998) 1189–1195.
[17] B. Korzeniewski, Biophys. Chem. 83 (2000) 19–34.

[18] B. Korzeniewski, J.-P. Mazat, Biochem. J. 319 (1996) 143–148.
[19] B. Korzeniewski, Mol. Cell. Biochem. 184 (1998) 345–358.
[20] A.K. Groen, R.J.A. Wanders, H.V. Westerhoff, R. van der Meer, J.M. Tager, J. Biol. Chem. 257 (1982) 2754–2757.
[21] D.F.S. Rolfe, J.M.B. Newman, J.A. Buckingham, M.G. Clark, M.D. Brand, Am. J. Physiol. 276 (1999) C692–C699.
[22] R.J.M. Henriksson, A. Katz, K. Sahlin, Biochem. J. 251 (1988) 183–187.
[23] M.K. Aliev, V.A. Saks, Biophys. J. 73 (1997) 428–445.
[24] M Vendelin, O. Kongas, V.A. Saks, Am. J. Physiol. 278 (2000) C747–C764.
[25] R.S. Balaban, H.L. Kantor, L.A. Katz, R.W. Briggs, Science 232 (1986) 1121–1123.
[26] R.S. Balaban, Am. J. Physiol. 258 (1990) C377–C389.
[27] L.A. Katz, J.A. Swain, M.A. Portman, R.S. Balaban, Am. J. Physiol. 256 (1989) H265–H274.
[28] B. Korzeniewski, Biochim. Biophys. Acta 1504 (2001) 31–45.
[29] F.W. Heineman, R.S. Balaban, Am. J. Physiol. 264 (1993) H433–H440.
[30] B. Saltin, J. Henriksson, E. Nygaard, P. Andersen, E. Jansson, in: P. Milvy (Ed.), The Marathon: Physiological, Medical, Epidemiological and Pathological Studies, 301, Annals of the New York Academy of Sciences, 1977, pp. 3–29.
[31] A.J. Sargeant, D.A. Jones, Fatigue, neural and muscular mechanismsin: S. Gandevia, R.M. Enoka, A.J. McComas, D.G. Stuart, C.K. Thomas (Eds.), Advances in Experimental Medicine and Biology, 384, Plenum, New York, 1995, pp. 323–338.
[32] P. Gollnick, K. Piehl, B. Saltin, J. Physiol. 241 (1974) 45–57.
[33] D.F.S. Rolfe, M.D. Brand, Biochim. Biophys. Acta 1276 (1996) 45–50.
[34] M. Tonkonogi, K. Sahlin, Acta Physiol. Scand. 161 (1997) 345–353.
[35] M.L. Blei, K.E. Conley, M.J. Kushmerick, J. Physiol. 465 (1993) 203–222.
[36] P. Andersen, B. Saltin, J. Physiol. 366 (1985) 233–249.
[37] E. Blomstrand, G. Radegran, B. Saltin, J. Physiol. 501 (1997) 455–460.
[38] T. Lettelier, M. Malgat, J.-P. Mazat, Biochim. Biophys. Acta 1141 (1993) 58–64.
[39] C.R. Taylor, Ann. Rev. Physiol. 49 (1987) 135–146.
[40] C.I. Funk, A. Clark, R.J. Connet, Am. J. Physiol. 258 (1990) C995–C1005.
[41] R.A. Meyer, Am. J. Physiol. 254 (1988) C548–C553.
[42] R.W. Wieseman, M.J. Kushmerick, J. Biol. Chem. 270 (1995) 12428–12438.
[43] E.W. McFarland, M.J. Kushmerick, T.S. Moerland, Biophys. J. 67 (1994) 1912–1924.
[44] M.J. Kushmerick, Comp. Biochem. Physiol. B 120 (1998) 109–123.
[45] T. Walliman, M. Wyss, D. Brdiczka, K. Nicolay, H.M. Eppenberger, Biochem. J. 281 (1992) 21–40.
[46] M. Wyss, J. Smeitink, R.A. Wevers, T. Walliman, Biochim. Biophys. Acta 1102 (1992) 119–166.
[47] J.W.R. Lawson, R.L. Veech, J. Biol. Chem. 254 (1979) 6528–6537.
[48] G.J. Kemp, D.J. Taylor, G.K. Radda, NMR Med. 6 (1993) 73–83.
[49] G.J. Kemp, C.H. Thompson, A.L. Sanderson, G.K. Radda, Magn. Reson. Med. 31 (1994) 103–109.
[50] B. Korzeniewski, W. Froncisz, Biochim. Biophys. Acta 1060 (1991) 210–223.
[51] M.J Kushmerick, R.A. Meyer, Am. J. Physiol. 248 (1985) C542–C549.
[52] H Hoppeler, Int. J. Sports Med. 7 (1986) 187–204.
[53] A. Zumstein, O. Mathieu, H. Howald, H. Hoppeler, Pflugers Arch. 397 (1983) 277–283.
[54] K. Sahlin, Biochemistry of exercise VIin: B. Saltin (Ed.), International Series on Sport Sciences, 16, Human Kinetics Publishers, Illinois, USA, 1986, pp. 323–343.
[55] K. Sahlin, M. Tonkonogi, K. Soderlund, Acta Physiol. Scand. 162 (1998) 261–266.
[56] J.A. Zoladz, Z. Szkutnik, J. Majerczak, K. Duda, Eur. J. App. Physiol. 78 (1998) 369–377.
[57] K.M. Brindle, M.J. Blackledge, R.A.J. Challiss, K.R. Radda, Biochemistry 28 (1989) 4887–4893.
[58] C.M. Sluse-Goffart, A. Evens, C. Duyckaerts, F.E. Sluse, in: H.V. Westerhoff, J.L. Snoep, J. Wijker, F.E. Sluse, B.N. Kholodenko (Eds.), BioThermoKinetics of the Living Cell, BioThermoKinetics Press, Amsterdam, 1996, pp. 218–224.
[59] M.J. Kushmerick, R.A. Meyer, T.R. Brown, Am. J. Physiol. 263 (1992) C598–C606.
[60] R.A. Meyer, J.M. Foley, Med. Sci. Sports Exerc. 26 (1994) 52–57.
[61] N.I. Kavanagh, E.K. Ainscow, M.D. Brand, Biochim. Biophys. Acta 1457 (2000) 57–70.